Selective studies of the excited rotational bands in the superdeformed nucleus ^{151}Tb

G. Benzoni,[1] J. Robin,[2] A. Bracco,[1] F. C. L. Crespi,[1] A. De Conto,[1] S. Leoni,[1] B. Million,[1] D. Montanari,[1] G. Duchêne,[2] D. Curien,[2] Th. Byrski,[2] F. A. Beck,[2] P. Bednarczyk,[2,*] S. Courtin,[2] O. Dorvaux,[2] B. J. P. Gall,[2] P. Joshi,[2] A. Nourreddine,[2] I. Piqueras,[2] J. P. Vivien,[2,†] and P. J. Twin[3]

[1]*Dipartimento di Fisica and INFN, Sezione di Milano, Milano, Italy*

[2]*Institut de Recherches Subatomiques, 23 rue du Loess, BP28 F-67037 Strasbourg, France*

[3]*Oliver Lodge Laboratory, University of Liverpool, Liverpool L69 7ZE, United Kingdom*

(Received 10 January 2007; published 6 April 2007)

The experimental study of the unresolved rotational bands, forming ridge structures in γ-γ spectra, has been performed on the superdeformed nucleus ^{151}Tb. γ transitions from the reaction ^{27}Al, at 155 MeV, on ^{130}Te were measured with EUROBALL IV in high fold coincidence. The analysis of the intensities and count fluctuations of the ridge structures shows the existence of $\approx$30 discrete rotational bands of superdeformed nature, half of which is in direct coincidence with the superdeformed yrast band. A comparison with band mixing model predictions and with a previous work on the superdeformed nucleus ^{143}Eu is presented.

DOI: 10.1103/PhysRevC.75.047301 PACS number(s): 21.10.Re, 23.20.Lv, 25.70.Gh, 27.70.+q

The study of the nuclear system at extreme conditions of excitation energy and angular momentum has improved our knowledge on the properties of highly excited nuclei, for which a theoretical description beyond mean field is required. The thermal response of the nucleus can be studied experimentally through the analysis of quasicontinuum spectra formed by rotational transitions among excited bands up to 4–5 MeV above yrast. This topic has been investigated mostly in normally deformed nuclei in inclusive ways and only limited information is available for selected nuclear configuration [1–3].

The thermal response of the nucleus in superdeformed systems is particularly interesting, since it is also influenced by the angular momentum which causes, for example, abrupt shape changes from superdeformed (SD) to spherical (ND) configurations. These studies require selective data obtained by gating on transitions collecting only few percents of the decay flow and associated to unresolved discrete rotational bands forming ridge structures in γ-γ matrices [1].

An interesting aspect concerning SD structures, not yet fully understood, is the decay out mechanism towards ND shapes. Almost all discrete SD bands observed so far [4] show a similar behavior: the intensity of the transitions is constant all the way down to the end of the band, dropping abruptly within few transitions. This sudden depopulation of the SD bands has been interpreted in terms of coupling to the compound ND states, coexisting over a wide spin range. In addition, the potential energy barrier separating the ND and SD configurations plays an important role in the decay-out process [5]. Therefore, the study of the rotational quasicontinuum can help establishing whether or not this mechanism can be extended to finite temperatures.

So far, experimental investigations of the SD rotational quasicontinuum concern only two nuclei in very different mass regions: ^{143}Eu and ^{194}Hg [3,6,7]. In the case of ^{143}Eu the ridge structures collecting the entire SD flow (not in direct coincidence with transitions of the SD yrast line) have been measured and well interpreted within a band mixing model also including the decay-out mechanism [8,9]. A number of bands ranging from 15 to 30 have been found, displaying a spreading in the moments of inertia of the order of 20%. In contrast, the analysis of ^{194}Hg has shown a much larger number of SD excited bands, of the order of 100–150, with a spreading in moment of inertia at least three times smaller than expected. This has been interpreted as a signature of ergodicity in a nuclear system [10].

The considerations above claim for additional studies to shed more light on the nature of the SD quasicontinuum and on its decay properties. A high statistics data set is available for the SD nucleus ^{151}Tb, which allows to study in great details, for the first time in this mass region, the SD ridge structures also in coincidence with the SD yrast band. In this Brief Report we report the results of this analysis together with comparisons with model predictions and with the previous work on ^{143}Eu.

The experiment has been performed at the Vivitron in Strasbourg (France). Terbium isotopes were produced by means of the reaction ^{27}Al impinging, at 155 MeV, on a stack of two self-supporting targets of ^{130}Te, each $\approx$500 μg cm^{-2} thick [11,12]. The subsequent γ-ray decays were measured using the EUROBALL IV array [13,14] in the standard configuration, having 15 Cluster detectors in the backward hemisphere, 26 Clover detectors at 90 degrees and 30 Tapered detectors in the forward hemisphere. An InnerBall of 210 BGO crystals was also present, allowing to determine the γ multiplicity of each single event. A fold selection of six unsuppressed (four suppressed) Ge detectors and ten BGO elements of the InnerBall firing in coincidence has allowed to collect $\approx 8.7 \times 10^9$ events of four- and higher-fold γ coincidences, in a total run time of 17 d. In the selected data ^{151}Tb was the main reaction channel, with a relative population of $\approx$77%. A detailed spectroscopy analysis of this nucleus has shown the existence of ten discrete rotational bands of large deformation ($\beta_2 \approx 0.6$), with intensities ranging between 6 to 30% of the

*Present address: GSI, Planckstrasse 1, D-64291, Darmstadt, Germany.

†Deceased.

SD yrast band, which has a relative yield of ≈2% [11,12,15]. The SD yrast band of ^{151}Tb is estimated to decay out at spin $69/2\hbar$. This value has been deduced from the analysis of the intensity and spin distribution of the ND states fed by the SD yrast band, since no linking transitions between the SD and ND states could be firmly established [11]. Such value is in agreement with the cranked mean field calculations of Ref. [16].

In order to study the global properties of the SD excited bands of ^{151}Tb, the data have been sorted into symmetric γ-γ matrices in coincidence with the isotope of interest, named *Total*, and in coincidence with the SD yrast band, named *SD*. In both cases a condition on high-fold events ($F \geqslant 20$) has been used in order to focus on high-multiplicity cascades, therefore enhancing the selection of SD structures. The *Total* matrix has been created requiring a single coincidence with the low-lying ND transitions at 268, 597.4, 604.5, and 615.9 keV, while the *SD* matrix has been created requiring a single gate on transitions belonging to the SD yrast band at the energies 854, 943, 988, 1081, 1129, and 1178 keV. In each case the corresponding background has been obtained scaling an ungated γ-γ matrix by a factor corresponding to the P/T of the gating transitions. This factor is ≈0.4 for the *Total* matrix and 0.02 for the *SD* one. In addition, the *Total* and *SD* matrices have been treated with the COR procedure [17], with a reduction factor of 0.85 and 0.4, respectively, in order to subtract the uncorrelated background still present.

In both matrices projections perpendicular to the main diagonal, $E_{\gamma_1} = E_{\gamma_2}$, reveal the existence of ridge structures of superdeformed nature: the spacing between the two most inner ridges, $2\Delta E_\gamma = 2 \times 4\hbar^2/\Im^{(2)} \approx 100$ keV, corresponds, in fact, to a moment of inertia, $\Im^{(2)}$, comparable to that of the known discrete SD bands, being $\Im^{(2)} \approx 80\hbar^2/\text{MeV}$ [4].

Examples of such spectra are given in Fig. 1: left panels show projections performed on the *Total* matrix and the right panels on the *SD* one. The panels are displayed in rows corresponding to the same average energy: top row $\langle E_\gamma \rangle =$ 1176 keV, middle row $\langle E_\gamma \rangle = 1228$ keV, and bottom row $\langle E_\gamma \rangle = 1280$ keV. The width of the projections is, in all cases, $\Delta E_\gamma \approx 50$ keV. In each panel the arrow indicates the position of the two most inner SD ridges. These ridge structures extend over a large range of γ transition energies, $900 < E_\gamma < 1400$ keV, corresponding to the spin interval $40 < I < 60\hbar$.

In all panels of Fig. 1 the dashed lines represent the full intensity spectra, while the solid lines show the intensity remaining after all known ND and SD discrete lines have been subtracted, making use of the RADWARE package [18,19]. The fact that the ridges stand out more clearly in the *SD* matrix than in the *Total* one depends on the SD-gating condition which selects more exclusively the SD structures.

The ridge structures are found to be populated by several unresolved discrete transitions, as confirmed in first place by the evaluation of their intensities and widths. Figure 2(a) shows the intensities of the SD ridges, both in the *Total* matrix (filled circles) and in the *SD* one (open circles). These values are compared to the intensity of the SD yrast band (filled squares), used as normalization. The intensity of the ridges closely resembles the SD-yrast pattern, showing a rather constant behavior below the feeding region

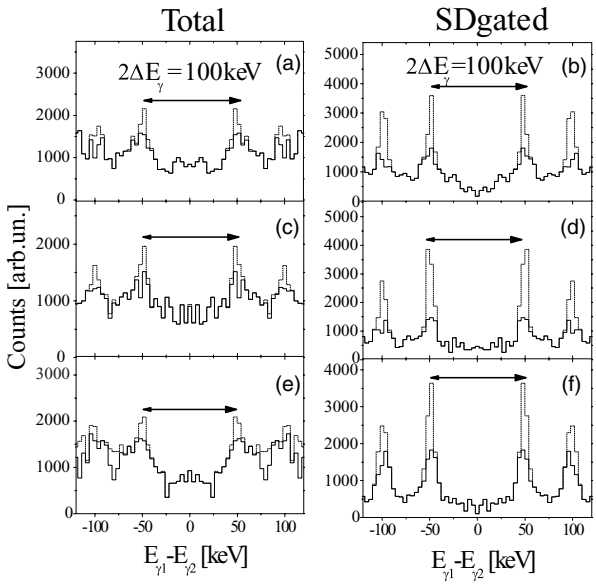

FIG. 1. Projections performed on the *Total* matrix (left panels) and on the *SD* one (right panels). The spectra correspond to the average energies 1176 keV [panels (a) and (b)], 1228 keV [panels (c) and (d)], and 1280 keV [panels (e) and (f)]. In all panels the arrow indicates the position of the most inner SD ridges, and the spacing $2 \times \Delta E_\gamma$ between them; the dashed lines represent the full intensity spectra, while the solid lines show the intensity remaining after the subtraction of all known discrete peaks.

($E_\gamma < 1300$ keV, $I < 57\hbar$). The analysis of the ridge structures could not be performed below 1100 keV ($I < 49\hbar$) owing to the presence of contaminations. In the case of the *Total* matrix the intensity of the ridges is up to three times larger than that of the SD yrast band, while the values obtained in direct coincidence with the SD band are instead only 1.5 times larger. This already indicates that no more than half of the SD excited bands are expected to remain in the SD minimum all the way down to the lowest spin values.

Figure 2(b) shows a comparison between the FWHM of the discrete lines and that of the SD ridges. It is found that the ridges observed in the *Total* and *SD* matrices (filled and open circles) have a similar width, of the order of 13 keV. This value is ≈3 times larger than the FWHM of the discrete lines of both SD and ND nature (filled and open squares), but ≈2 times smaller than the typical FWHM of ridge structures populated by ND rotational nuclei [1]. Since the width of the ridge is related to the dispersion in moment of inertia of the rotational bands populating this structure, narrower ridges are expected in strongly elongated nuclei, generally characterized by rotational bands with similar dynamic moments of inertia. This is also true in the case of the known SD bands of ^{151}Tb [12,15]. It is worth noticing that the 13 keV value here obtained for the FWHM of the SD ridges (corresponding to ≈20% spreading in the $\Im^{(2)}$ moment of inertia) is consistent with the analysis performed in the neighboring SD nucleus ^{143}Eu [3], while it is definitely larger than the 8 keV value reported in the case of ^{194}Hg [7]. This observation, together with the large difference in number of bands populating the ridges (lately discussed), points to different properties of the excited

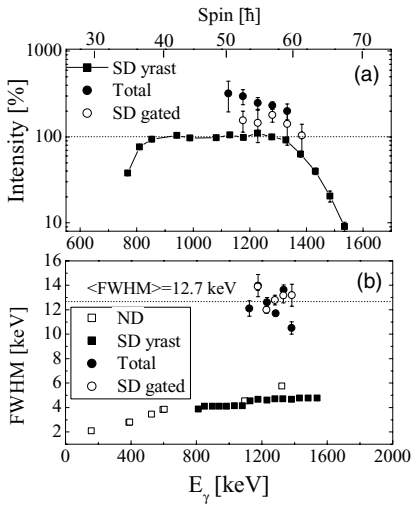

FIG. 2. Panel (a) shows the intensities of the SD ridges in the *Total* (filled circles) and in the *SD* matrix (open circles) as function of E_γ (the top axis gives the spin correspondance). Panel (b) shows the FWHM of the discrete transitions, of SD and ND nature (filled and open squares) and of the SD ridge structures (filled and open circles). The dotted line gives the average FWHM obtained from the analysis of the ridges.

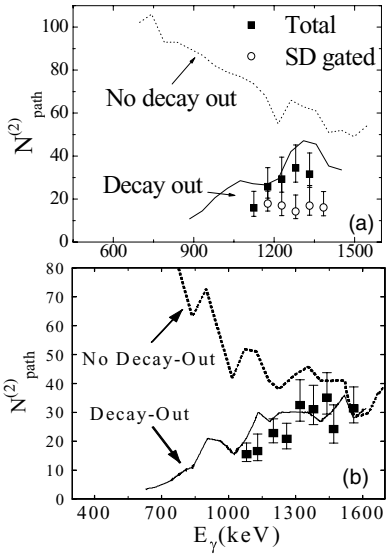

FIG. 3. Comparison between the experimental number of SD paths (symbols) and cranked shell model calculations (lines), for ^{151}Tb [panel (a)] and ^{143}Eu [panel (b)] [3]. For ^{151}Tb, the filled (open) symbols refer to the analysis of the *Total* (*SD* gated) matrix. For ^{143}Eu only the total number of decay paths is available. In both panels the dashed lines refer to the model of Ref. [8], which does not take into account the decay out towards ND states. The full lines show predictions including also a probability to decay into the ND well [9]. In the case of ^{151}Tb, the calculations assume (in the decay-out spin region) the average decay-out probability $\langle P_{\text{out}} \rangle$ obtained in the case of ^{143}Eu in the corresponding decay-out spin region (see text).

SD bands in the mass region $A = 140$–150 as compared to the heavier system ^{194}Hg, where the exceptionally narrow ridges have been attributed to ergodic bands, namely collective rotational states of chaotic nature [10].

In order to provide information on the dynamics of the γ decay in the SD well and on the coupling with the ND states, we evaluated the number of bands populating the SD ridge structures, making use of the fluctuation analysis of the counts in a γ-γ coincidence matrix [20]. The number of bands is given by the expression

$$N^{(2)}_{\text{path}} = \frac{N_{\text{eve}}}{\frac{\mu_2}{\mu_1} - 1} \times P^{(2)}, \tag{1}$$

where N_{eve}, μ_1 and μ_2 are the intensity, the first and second moments of the distribution of counts in the ridge, while $P^{(2)}$ is a factor that accounts for the experimental resolution. The superscript $^{(2)}$ indicates that we are considering cascades made of two consecutive transitions. Owing to the richness of this data set statistically meaningful fluctuations could be obtained, for the first time, even for the ridge structures in the *SD* matrix.

The results of the fluctuation analysis on ^{151}Tb are shown in Fig. 3(a): up to ≈30 bands are found to populate the SD ridges (filled squares), ≈15 of which in direct coincidence with the SD yrast band (open circles). This is consistent with the factor of 2 difference already observed between the intensity of the *Total* and SD-gated ridges [Fig. 2(a)]. While the total number of SD bands shows a marked decrease with decreasing spin/transition energy (as a consequence of the decay out towards ND states), the number of bands in direct coincidence with the SD yrast band is constant, since these bands decay only through the SD yrast band itself. The fact that the total ridge intensity stays constant below $E_\gamma \approx 1200$ keV, while the $N^{(2)}_{\text{path}}$ decreases, is due to a stronger population of these few excited bands, which are closer to yrast.

Figure 3(b) shows for comparison the analysis of the total SD ridges of the nucleus ^{143}Eu, reported in Ref. [3]. As one can see, the experimental values obtained in the two cases are rather similar, in terms of both absolute numbers and general trend. This suggests very similar properties for the unresolved excited bands in the two nuclei of mass $A = 140$–150, at variance from the case of ^{194}Hg, where more than 100 SD bands have been observed to populate extremely narrow ridges, confirming the different nature of these unresolved states [7,10].

The interpretation of the results of the fluctuation analysis of the SD ridge structures of ^{151}Tb has been based on the cranked shell model calculations discussed in Refs. [8,9], successfully employed in the case of the SD nucleus ^{143}Eu. The model calculates, for each parity and spin, the microscopic levels and $E2$ transition probabilities up to few MeV above yrast, combining a cranked Nilsson mean field and a residual two-body interaction. One can therefore obtain, at each given spin, the number of discrete excited bands, by counting, at increasing excitation energy above yrast, the number of bands which fragment to less than two states. As shown in Figs. 3(a) and 3(b) by dashed lines, the model largely overestimates the experimental data in both nuclei, especially at low transition energies, where the experimental number of decay paths decreases presumably as a consequence of the decay out towards ND structures. A better agreement between theory and experiment is obtained once we take into account,

for each SD excited band, a probability to decay towards ND states.

According to the model described in Ref. [9], the average probability to decay out of the SD well, $\langle P_{\text{out}} \rangle$, can be evaluated, in the weak coupling limit, when $\Gamma_t / D_{ND} < 1$, by the expression

$$\langle P_{\text{out}} \rangle = \sqrt{\pi/2} * \sqrt{\frac{\Gamma_t}{D_{ND}} * \frac{\Gamma_{ND}}{\Gamma_{SD}}}, \tag{2}$$

where D_{ND} is the level spacing of ND states, Γ_{ND} and Γ_{SD} are the electromagnetic decay widths and Γ_t is the tunneling probability through the potential energy barrier between the ND and SD well.

The predictions for the total number of paths obtained taking into account decay-out probability $\langle P_{\text{out}} \rangle$ for each SD excited band have been found to reproduce well the experimental results for the nucleus ^{143}Eu, as shown in Fig. 3(b) by the solid line. In the case of ^{151}Tb, since no calculations are presently available, we have estimated the expected number of decay paths (including the decay-out mechanism) using, in the spin region above the decay out (i.e., $I \geqslant 69/2\,\hbar$, $E_\gamma \geqslant 700$ keV), the $\langle P_{\text{out}} \rangle$ values calculated for ^{143}Eu in the corresponding decay-out region (i.e., $I \geqslant 34/2\hbar$, $E_\gamma \geqslant 500$ keV) [21]. This is justified by the fact that the two nuclei lie in the same mass region and the main quantities entering in the evaluation of $\langle P_{\text{out}} \rangle$ are not expected to differ significantly. The obtained results are shown in Fig. 3(a) by the solid line, and a rather good agreement with the data (symbols) is in fact achieved.

One can then conclude that the decay-out mechanism modelled as in the case of the SD yrast states is an essential ingredient to interpret the experimental results in the mass region $A = 140$–150. For a more detailed interpretation of the component of the SD continuum populating directly the SD yrast band, and of the decay out in the feeding region, more refined calculations are needed. It should also be noticed that the present results provide information on the composition of the superdeformed continuum and therefore they can be used to further test several ingredients of the decay-out process, such as the barrier height and width and the inertial mass parameter, which is driven by pairing.

Discussions with E. Vigezzi, M. Matsuo, and Y. R. Shimizu are gratefully acknowledged. This work was partially supported by the EU (Contract No. EUROVIV: HPRI-CT-1999-00078) and by the Italian Istituto Nazionale di Fisica Nucleare.

[1] A. Bracco and S. Leoni, Rep. Prog. Phys. **65**, 299 (2002).
[2] G. Benzoni *et al.*, Phys. Lett. **B615**, 160 (2005).
[3] S. Leoni *et al.*, Phys. Lett. **B498**, 137 (2001).
[4] B. Singh *et al.*, Nucl. Data Sheets **97**, 241 (2002).
[5] B. Herskind *et al.*, Phys. Rev. Lett. **59**, 2416 (1987).
[6] S. Leoni *et al.*, Phys. Lett. **B409**, 71 (1997).
[7] A. Lopez-Martens *et al.*, Eur. Phys. J. A **20**, 49 (2004).
[8] K. Yoshida and M. Matsuo, Nucl. Phys. **A612**, 26 (1997).
[9] K. Yoshida, M. Matsuo, and Y. R. Shimizu, Nucl. Phys. **A696**, 85 (2001).
[10] M. Matsuo *et al.*, AIP Conf. Proc. **701**, 157 (2004).
[11] G. Duchêne *et al.*, AIP Conf. Proc. **701**, 222 (2004).
[12] J. Robin *et al.* (to be published).
[13] F. A. Beck, Prog. Part. Nucl. Phys. **28**, 43 (1992); J. Simpson, Z. Phys. A **358**, 139 (1997).
[14] Achievements with the Euroball spectrometer, Scientific and Technical activity Report 1997–2003, edited by W. Korten and S. Lunardi.
[15] B. Kharraja *et al.*, Phys. Lett. **B341**, 268 (1995).
[16] I. Ragnarsson, Nucl. Phys. **A557**, 167c (1993).
[17] O. Andersen *et al.*, Phys. Rev. Lett. **43**, 687 (1979).
[18] D. C. Radford, Nucl. Instrum. Methods Phys. Res. A **361**, 297 (1995).
[19] D. C. Radford, Nucl. Instrum. Methods Phys. Res. A **361**, 306 (1995).
[20] T. Døssing *et al.*, Phys. Rep. **268**, 1 (1996).
[21] A. Atac *et al.*, Phys. Rev. Lett. **70**, 1069 (1993).